Autosomal Dominant Hypoparathyroidism Caused by Germline Mutation in *GNA11*: Phenotypic and Molecular Characterization

Dong Li, Evan E. Opas, Florin Tuluc, Daniel L. Metzger, Cuiping Hou, Hakon Hakonarson, and Michael A. Levine

Center for Applied Genomics (D.L., C.H., H.H.), Division of Endocrinology and Diabetes (E.E.O., M.A.L.), Division of Allergy and Immunology (F.T.), Division of Pulmonary Medicine (H.H.), and Center for Bone Health (M.A.L.), The Children's Hospital of Philadelphia; and Department of Pediatrics (H.H., M.A.L.), University of Pennsylvania Perelman School of Medicine, Philadelphia, Pennsylvania 19104; and Endocrinology and Diabetes Unit (D.L.M.), British Columbia Children's Hospital, and Department of Pediatrics (D.L.M.), University of British Columbia, Vancouver, British Columbia, Canada V5Z 4H4

Context: Most cases of autosomal dominant hypoparathyroidism (ADH) are caused by gain-of-function mutations in *CASR* or dominant inhibitor mutations in *GCM2* or *PTH*.

Objective: Our objectives were to identify the genetic basis for ADH in a multigenerational family and define the underlying disease mechanism.

Subjects: Here we evaluated a multigenerational family with ADH in which affected subjects had normal sequences in these genes and were shorter than unaffected family members.

Methods: We collected clinical and biochemical data from 6 of 11 affected subjects and performed whole-exome sequence analysis on DNA from two affected sisters and their affected father. Functional studies were performed after expression of wild-type and mutant $G\alpha_{11}$ proteins in human embryonic kidney-293-CaR cells that stably express calcium-sensing receptors.

Results: Whole-exome-sequencing followed by Sanger sequencing revealed a heterozygous mutation, c.179G>T; p.R60L, in *GNA11*, which encodes the α-subunit of G_{11}, the principal heterotrimeric G protein that couples calcium-sensing receptors to signal activation in parathyroid cells. Functional studies of $G\alpha_{11}$ R60L showed increased accumulation of intracellular concentration of free calcium in response to extracellular concentration of free calcium with a significantly decreased EC_{50} compared with wild-type $G\alpha_{11}$. By contrast, R60L was significantly less effective than the oncogenic Q209L form of $G\alpha_{11}$ as an activator of the MAPK pathway. Compared to subjects with *CASR* mutations, patients with *GNA11* mutations lacked hypercalciuria and had normal serum magnesium levels.

Conclusions: Our findings indicate that the germline gain-of-function mutation of *GNA11* is a cause of ADH and implicate a novel role for *GNA11* in skeletal growth. **(*J Clin Endocrinol Metab* 99: E1774–E1783, 2014)**

Hypoparathyroidism is characterized by hypocalcemia and hyperphosphatemia due to inadequate supply or effectiveness of circulating PTH. It may be present either as an isolated finding or as a component of a more complex developmental, metabolic, or endocrine syndrome. Molecular genetic studies indicate that isolated hypoparathyroidism is caused by mutations in a variety of genes, including genetic defects that impair synthesis [ie,

ISSN Print 0021-972X ISSN Online 1945-7197
Printed in U.S.A.

Received January 6, 2014. Accepted May 5, 2014.
First Published Online May 13, 2014

Abbreviations: AM, tetra(acetoxymethyl)-ester; $[Ca^{2+}]_o$, concentration of extracellular calcium; CaSR, calcium-sensing receptor; FEca, fractional excretion of calcium; HBSS, Hanks' balanced salt solution; HEK293, human embryonic kidney 293; JNK, c-Jun N-terminal kinase; MARCKS, myristoylated alanine-rich C-kinase substrate; PI-PLC, phosphoinositol-specific phospholipase C; SRE, serum response element; WES, whole-exome sequencing.

PTH (1)] or secretion [ie, *CASR* (2, 3)] of PTH as well as defects that impair the embryological development of the parathyroid glands [*GCM2* (4)]. Gain-of-function mutations in the *CASR* gene located on chromosome 3q13.3-q21 are the most common genetic cause of isolated hypoparathyroidism (5) and result in a disorder that is also termed autosomal dominant hypocalcemia (6).

The *CASR* gene encodes the calcium-sensing receptor (CaSR), a G protein-coupled receptor that is expressed abundantly in the parathyroid and, to a lesser extent, along the length of the kidney tubule. The CaSR plays a central role in calcium homeostasis by sensing the concentration of extracellular calcium ($[Ca^{2+}]_o$); activation of the CaSR-coupled signaling pathways inhibits PTH secretion and reduces calcium reabsorption in the distal nephron. Patients with gain-of-function mutations in the *CASR* manifest varying degrees of hypocalcemia with inappropriately low circulating PTH levels and relative hypercalciuria, features that are explained by the expression of CaSRs with increased sensitivity to calcium in the parathyroid gland and the distal renal tubule (3) and that distinguish these patients from subjects with other forms of hypoparathyroidism (7). The critical importance of the CaSR signaling pathway in controlling parathyroid function has recently been extended through the description of patients with hypoparathyroidism who have gain-of-function mutations in *GNA11* (8, 9), which encodes the α-subunit of G_{11}, the principal G protein that transduces CaSR signaling in the parathyroid.

In the present study, we analyzed members of a previously described multigenerational kindred with autosomal dominant transmission of isolated hypoparathyroidism and short stature (10). This kindred was originally ascertained through a proband who also had nephrogenic diabetes insipidus. Although these features suggested autosomal dominant hypocalcemia, our sequence analysis of the *CASR, PTH*, and *GCM2* genes, which encode the calcium sensing receptor, PTH, and glial cells missing homolog 2, respectively, in affected subjects did not disclose a mutation. Here we report the use of whole-exome sequencing (WES) in members of this kindred and describe a germline heterozygous mutation of *GNA11* that leads to a gain of function as the basis for autosomal dominant hypoparathyroidism.

Patients and Methods

Patients

We isolated genomic DNA from blood or saliva obtained from members of the family described by Hunter et al (10), including two affected brothers (III-13 and III-15; Figure 1A), their affected mother (II-8) and children (IV-3–5), and III-13's unaffected wife (III-14). Other members of this family refused to participate. The affected subjects had biochemical hypoparathy-

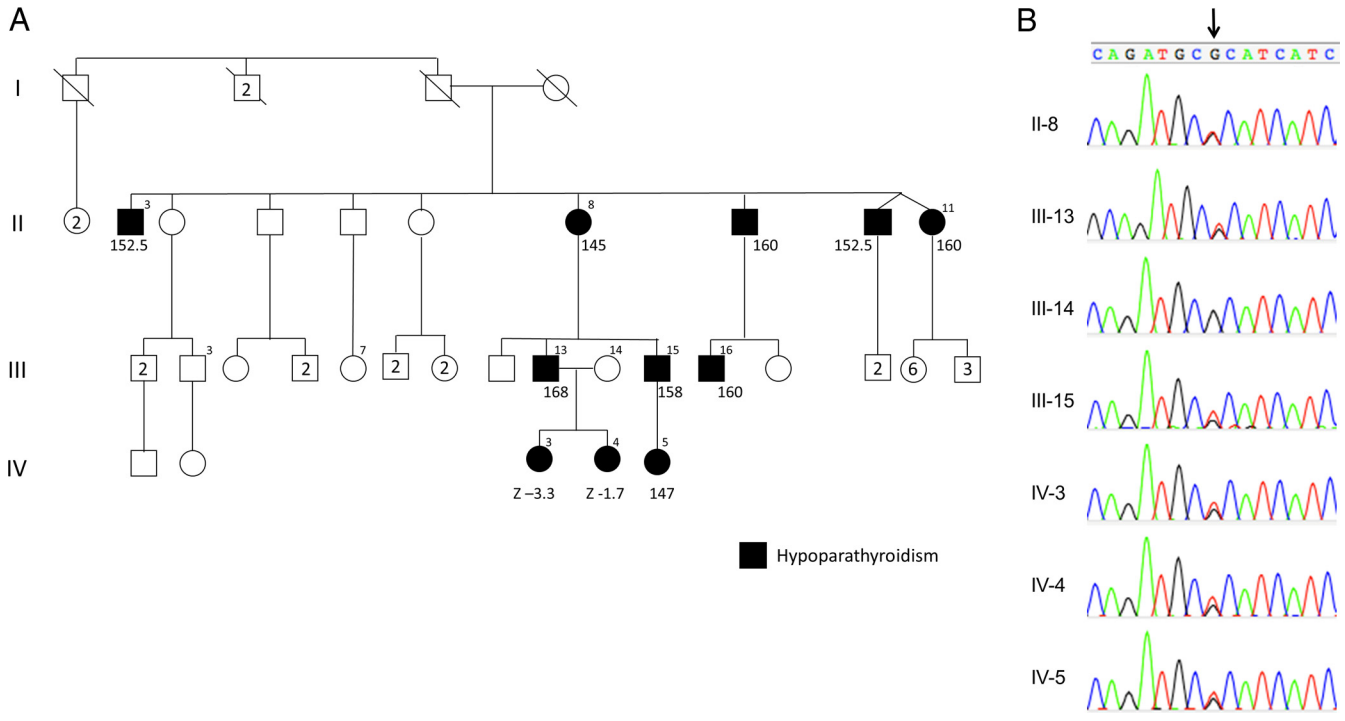

Figure 1. Pedigree of the studied family and confirmation of the *GNA11* mutation. Panel A shows the pedigree of the family with familial hypoparathyroidism. Squares represent male family members, circles female family members, and black symbols affected family members. The height of each affected subject is below the symbol, either as centimeters or Z score. Panel B shows the sequencing chromatograms for direct sequence analysis of amplicons of exon 2 of *GNA11*. Sanger sequencing confirmed the presence of the heterozygous c.179G>T (p.R60L) missense mutation in all affected subjects.

roidism with low concentrations of serum calcium and intact PTH and elevated concentrations of serum phosphorus. Eight other unrelated subjects with hypoparathyroidism due to activating mutations of the *CASR* (E799K, F832S, F854Y/A844V, E604K, S820Y) provided biochemical data. These subjects were ascertained nonrandomly from five unrelated families and were aged 3–48 years. At diagnosis, all subjects had low or low normal levels of PTH, hypocalcemia, and hyperphosphatemia. Four of eight subjects have passed renal stones and two additional subjects have nephrocalcinosis. All subjects provided written informed consent/assent for participation in the study. The study was approved by the Institutional Review Board at The Children's Hospital of Philadelphia.

Prior mutation screening

Mutation screenings of the *CASR, PTH*, and *GCM2* genes were performed by Sanger sequencing the exons and exon-intron boundaries but failed to identify any deleterious disease-causing mutations.

Exome sequencing and bioinformatic analysis

The exome was captured for three affected patients, III-13, IV-3, and IV-4, using the Aglient SureSelect Human All Exon version 3 kit (Agilent Technologies), guided by the manufacturer's protocols. All the raw reads were aligned to the reference human genome using the Burrows-Wheeler Aligner (BWA) (11) and single-nucleotide variants and small insertions/deletions were captured using the genome analysis tool kit (GATK) (12). ANNOVAR (13) and SnpEff (14) were subsequently used to functionally annotate the variants. Under the autosomal dominant mode of inheritance, we excluded variants with the following factors: 1) were synonymous variants; 2) had a minor allele frequency of greater than 0.005 in the 1000 Genomes Project, 6503 exomes from the National Heart, Lung, and Blood Institute Exome Sequencing Project (ESP6500SI; http://evs.gs.washington.edu/EVS/), or our in-house database of greater than 1200 sequenced exomes; 3) had a conservation score Genomic Evolutionary Rate Profiling + + less than 2; and 4) were predicted by Sorting Intolerant From Tolerant/Polymorphism Phenotyping v2 scores to be benign variants. Validation of the mutation candidate was performed by Sanger sequencing in all available family members.

The structure of wild-type $G\alpha_{11}$ and $G\alpha_{11}$-R60L was modeled with PyMod plug-in (v.1.0b) (Schrödinger) (15) using the crystal structures of $G\alpha_q$ (Protein Data Bank accession numbers 3OHM and 3AH8) (16) and examined with PyMOL software (v.1.1r1) (Schrödinger).

Biochemical analyses

The cDNAs corresponding to wild-type *GNA11* and the Q209L activating mutation (17) were obtained in the pLENTI6.2/TO/V5 vector from Dr Boris C. Bastian (Department of Pathology, University of California, San Francisco, San Francisco, California). These cDNAs contain altered residues at positions GYLPTQ to EYMPTE to create internal Glu-Glu epitope tags and retain full function. The R60L substitution was engineered by site-directed mutagenesis of wild-type *GNA11* and was sequenced for confirmation. A reporter plasmid in which an improved destabilized firefly luciferase is under the control of the serum response element (SRE)-*luc2CP* (18) was a generous gift of Dr Frank Fan (Department of Research, Promega Corp, Madison, Wisconsin). We obtained a human embryonic kidney 293 (HEK293) cell line that stably expresses the human CaSR (HEK293-CaSR) from Dr Aldebaran M. Hofer (Brigham and Women's Hospital, Boston, Massachusetts). Transient transfections were performed using FuGENE 6 (Roche); transfection efficiencies were typically 50%–70%. For luciferase reporter assays, HEK293-CaSR cells were transfected in 24-well plates using 200 ng $G\alpha_{11}$ plasmid or empty vector, plus 10 ng of the pRL *Renilla* luciferase reporter and 200 ng of the SRE reporter. The cells were changed to serum-starving medium 24 hours after transfection. The following day, the medium was replaced with 20 mM HEPES (pH 7.4), 125 mM NaCl, 4.0 mM KCl, 0.5 mM $MgCl_2$, and 0.1% D-glucose, with 1 mg/mL BSA containing various $[Ca^{2+}]_o$. Luciferase activity was assayed using the Promega dual-reporter assay system. Firefly luciferase activity was normalized to the *Renilla* luciferase activity.

To determine phosphorylation of ERK1/2, p38, c-Jun N-terminal kinase (JNK), and phosphorylated AKT in HEK293-CaSR cells that had been transfected with $G\alpha_{11}$ plasmids or empty vector, we performed immunoblot analysis on cell lysates that had been sonicated and cleared by centrifugation. Equal amounts (15 μg) of protein were subjected to 4%–12% SDS-PAGE, and blots were subsequently incubated with polyclonal antibodies that specifically recognize phosphorylated forms of p44/42 MAPK (ERK1/2), p38 MAPK, Akt, myristoylated alanine-rich C-kinase substrate (MARCKS), and JNK. Antibody binding was detected using a second antibody that was labeled with horseradish peroxidase and a chemiluminescence method. Primary antibodies against $G\alpha_{q/11}$ (Santa Cruz Biotechnology) and EE (Covance) were used to assess the expression of the $G\alpha_{11}$ proteins, and anti β-actin (Sigma) was used to verify equal loading of all lanes with total protein. All assays and immunoblots were performed using independent lysates derived from triplicate-well transfections for each condition, and the data that are presented represent the results of three to five separate experiments.

Intracellular calcium measurements

Transfected HEK293-CaSR cells were grown in six-well plates, detached, resuspended in Hanks' balanced salt solution (HBSS), and simultaneously loaded with Fluo-4 tetra(acetoxymethyl)-ester (AM; 2 μM) and Fura red AM (2 μM) for 45 minutes at room temperature. Cells were washed in HBSS containing calcium chloride (0.1 mM). Aliquots (50 μl) of suspended cells were mixed with an equal volume of HBSS containing calcium chloride to yield final calcium concentrations of 0.3, 0.6, 1, 1.8, 3.2, 5.6, or 10 mM. Immediately after mixing, each cell sample was analyzed on an Accuri C6 flow cytometer (BD Biosciences). The ratio between fluorescence intensities recorded in the FL-1 channel (530/30 nm; Fluo-4 AM) and the FL-3 channel (670 nm long pass; Fura-red AM) was calculated for each cell as a derived parameter using FlowJo 7.6.5. (Tree Star Inc). Curves were fitted to data using the four-parameter Hill equation (19). EC_{50} values were determined for each cell type tested, and the mean EC_{50} values were calculated from data obtained from four sets of measurements.

Results

Clinical and biochemical characteristics of the family

We were able to obtain DNA and additional clinical information from two affected brothers (III-13 and III-15)

of the original proband (III-16; Figure 1A) described by Hunter et al (10) as well as from their affected mother (II-8). The proband (Figure 1A, individual III-16) was originally described as having nephrogenic diabetes insipidus when he presented with hypoparathyroidism as a child (10). The basis for this episode of transient diabetes insipidus remains unknown, and no other member of the extended family has ever manifested symptoms of diabetes insipidus. Subject II-8 has a history of transient hypercalcemia and nephrocalcinosis due to an episode of vitamin D intoxication but has had normal urinary calcium excretion, whereas her serum calcium was normal. Subjects IV-3 and IV-4 were diagnosed in infancy based on their father's known diagnosis, whereas subject IV-5 had previously refused biochemical screening and was diagnosed at age 20 years after experiencing an episode of severe tetany. In Table 1 we present detailed biochemical data from four affected subjects (Figure 1A, III-13, IV-3, IV-4, and IV-5) compared with eight subjects with activating mutations of the *CASR*. Subjects III-13, IV-3, and IV-4 had normal serum concentrations of magnesium and low or normal fractional excretion of calcium (FEca) and urinary calcium to creatinine ratios while hypocalcemic and normocalcemic, both before and during treatment with calcitriol plus calcium. A remarkable feature of this family is that affected members develop mild postnatal growth failure without evidence of GH deficiency (data not shown) and are significantly shorter than their unaffected relatives [Figure 1A, Table 1, and Table 2 and Hunter et al (10)].

Table 2. Adult Heights of Affected and Unaffected Members of This Kindred

	Affected (n)	Unaffected (n)	*P* Value
Adult male	158.2 ± 6.4 (5)	170.2 ± 7.4 (6)	<.02
Adult female	149.0 ± 2.6 (3)	164.1 ± 3.5 (4)	<.01

Family-based exome sequencing and bioinformatics analysis

We performed WES on three affected patients (III-13, IV-3, and IV-4). The exome variant profile was considered under the assumption of an autosomal dominant model based on family history. A total of 47 421 single-nucleotide variants and 3847 insertions/deletions were identified in the three samples, of which 46 010 (97.0%) and 2527 (65.7%) were reported in build 135 of the dbSNP relational database of single nucleotide polymorphisms. As described in *Patients and Methods*, we filtered variants to exclude those that had a minor allele frequency greater than 0.5% or predictive of benign variant. This process left only 15 candidates (Supplemental Table 1), among which c.179G>T (p.R60L) in *GNA11* was selected as the most likely disease-causing candidate because G_q and G_{11} are known to couple the CaSR to calcium-dependent activation of intracellular signaling pathways that decrease the rate of PTH secretion from the parathyroid cell (20). This mutation (p.R60L) is present in all members of the $G\alpha_{q/11}$, $G\alpha_{12/13}$, and $G\alpha_s$ families. The cosegregation of the mutation with phenotype was confirmed by Sanger sequencing (Figure 1B) demonstrating the presence of the heterozygous R60L in these three patients as well as in three additional affected patients (II-8, III-15, and IV-5) and the absence in III-13's unaffected wife. Although other unaffected subjects from this family were not willing to participate in the study and provide us with DNA samples, the analysis of existing sequencing data from more than 1200 WES samples in our database did not detect another occurrence of this mutation.

Previous molecular modeling showed that Arg60 is a critical residue within the α1 helix of $G\alpha_{11}$ (and $G\alpha_q$) that forms a salt bridge with Asp71 from the helical domain (αA helix) (16). This Arg-Asp pair stabilizes linker 1, which together with switch I (linker 2), stabilize the helical and Ras-like GTPase domains of Gα that act like a clam shell to bury the GDP nucleotide and its associated mag-

Table 1. Biochemical Features of Four Affected Subjects[a]

	Age, y	Calcium, mmol/L	Phos, mmol/L	Mag, mmol/L	PTH, pmol/L	FEca, %
III-13	42	1.86	1.8	0.89	2.1	1.88
IV-3	9	1.94 ± 0.11	2.27 ± 0.16	0.79 ± 0.06	0.6	0.24
IV-4	14	1.85 ± 0.08	2.40 ± 0.22	0.80 ± 0.05	1.2	0.35
IV-5	20	1.78 ± 0.01			1.3	1.17
GNA11 mutations (mean ± SD)						0.91 ± 0.77[b]
CASR-activating mutations (n = 8, mean ± SD)						2.70 ± 0.98
Normal		2.20–2.60	0.8–1.8	0.7–1.0	1.2–5.8	1.0–2.0

Abbreviations: Mag, magnesium; Phos, phosphorus.

[a] Serum biochemistries for the four affected subjects are presented as the mean ± SD for two to 10 values.

[b] The two-tailed value is $P < .03$ for comparison between subjects with *GNA11* mutations and *CASR* mutations.

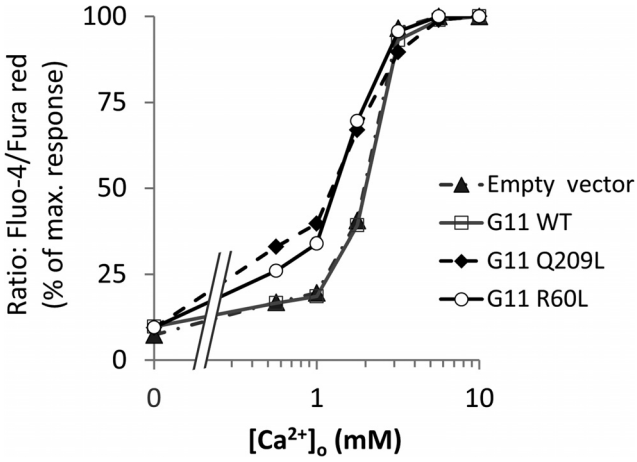

Figure 2. Effects of *GNA11* mutants on the EC_{50} for extracellular calcium in calcium-sensing receptor-expressing cells. The figure shows the responses of intracellular calcium concentrations to changes in extracellular calcium concentrations in HEK293 cells stably expressing calcium-sensing receptors were transiently transfected with an empty expression plasmid vector or plasmids expressing $G\alpha_{11}$ cDNAs corresponding to the wild-type or mutant (R60L or Q209L) sequences. The intracellular calcium responses to changes in extracellular calcium concentrations are expressed as a percentage of the maximum normalized response and are shown as the mean value. The mutant $G\alpha_{11}$ cDNAs produced leftward shifts in the concentration-response curve, with significantly lower EC_{50} values (see text). The figure is representative of three independent experiments with similar results.

nesium ion. Replacement of arginine by leucine disrupts this salt bridge (Supplemental Figure 1), thereby increasing the inherent flexibility of the linker 1 region that connects the helical and GTPase domains of the α-subunit and promoting a more open state for the clam shell that facilitates GDP-GTP exchange (21).

Effect of the *GNA11* mutations on intracellular calcium accumulation

Expression of $G\alpha_{11}$ was significantly increased in cells transfected with wild-type or mutated $G\alpha_{11}$ cDNAs, whereas expression of $G\alpha_q$ was unchanged (Supplemental Figure 2). The $G\alpha_{11}$ mutant, R60L, as well as the Q209L protooncogene, resulted in similar leftward shifts in the concentration-response curves, with significantly lower ($P < .02$) EC_{50} values (1.22 ± 0.14 mM and 1.16 ± 0.18 mM, respectively), as compared with wild-type $G\alpha_{11}$ (1.82 ± 0.28 mM) or empty vector (1.82 ± 0.15 mM; Figure 2). The decreased EC_{50} value for $[Ca^{2+}]_o$ that is induced by the R60L mutant indicates an enhanced sensitivity of cells expressing CaSRs to changes in extracellular calcium concentrations and is consistent with a gain-of-function mutation.

Effect of the *GNA11* mutations on mitogenic signaling pathways

Somatic missense mutations that replace Q209 and R183 in both *GNA11* and *GNAQ* are considered protooncogenic and have been identified in some blue nevi, primary uveal melanomas, uveal melanoma metastases, and central nervous system melanocytomas (17, 22) as well as port-wine stains and Sturge-Weber syndrome (23). These mutations induced spontaneously metastasizing tumors in a mouse model and activated the MAPK pathway. As shown in Figure 3A, HEK293-CaSR cells that had been transfected with $G\alpha_{11}$ Q209L showed significantly ($P < .05$) greater activation of ERK1/2, as indicated by increased phosphorylation, compared with cells that had been transfected with R60L, which was only slightly more active than either wild-type $G\alpha_{11}$ or the empty vector. There was no significant difference in the EC_{50} for $[Ca^{2+}]_o$ for Q209L, R60L, or wild-type $G\alpha_{11}$ proteins. By contrast, the efficacy (ie, the maximal response to calcium) was significantly greater for Q209L than for R60L or wild-type $G\alpha_{11}$ (Figure 3B).

Activation of the ERK/MAPK pathway can induce transcriptional activation by various response elements including the SRE. SRE-mediated gene transcription is known to

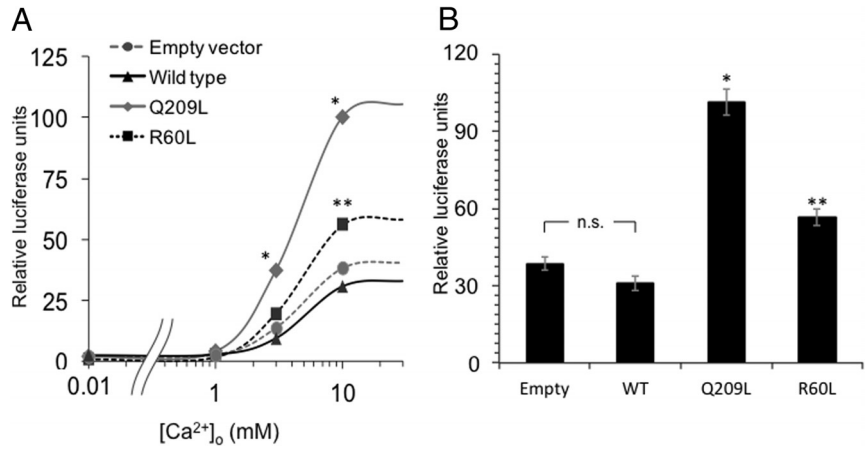

Figure 3. Activation of MAPK activity by GNA11. HEK293 cells stably expressing calcium-sensing receptors were transiently transfected with an empty expression plasmid vector or plasmids expressing $G\alpha_{11}$ cDNAs corresponding to the wild-type or mutant (R60L or Q209L) sequences. We assessed $G\alpha_{11}$-dependent activation of MAPK by measuring the phosphorylation of ERK (pERK) by semiquantitative immunoblot analysis. The pERK responses to changes in extracellular calcium concentrations are expressed as arbitrary units and are shown as the mean (±SE) value from three experiments. Panel A shows the complete concentration curve, with lower EC_{50} values for the Q209L (3.77 mM) and R60L (3.78 mM) mutants compared with the wild type (4.47 mM) or empty vector (4.01 mM). Panel B depicts efficacy in response to 10 mM extracellular calcium. There was significantly greater phosphorylation of ERK with $G\alpha_{11}$ p.Q209L (*, $P < .02$ vs R60L; $P < .003$ vs WT and Empty) than p.R60L (**, $P < .02$ vs WT and $P < .04$ vs empty vector). There was no significant difference (P = n.s.) between the wild type and empty vector. WT, wild type.

be rapidly induced by serum, phorbol esters, and growth factors and can be assessed in a promoter reporter assay (18). Figure 4A shows that HEK293-CaSR cells expressing the wild-type $G\alpha_{11}$ and empty vector had similar EC_{50} values for calcium responsiveness (3.26 mM vs 3.76 mM), whereas cells expressing the R60L had a significantly ($P < .05$) lower EC_{50} (2.74 mM) value. By contrast, cells expressing the Q209L (EC_{50} 2.65 mM) $G\alpha_{11}$ showed marked activation of SRE reporter activity, even in the absence of extracellular calcium, with only a modest increase in activity upon the addition of calcium (Figure 4A). Cells responded to incubation with 10 mM calcium with increased ($P < .05$) phosphorylation of p38 and MARCKS. Moreover, the Q209L mutant strongly activated the p38 and JNK mitogenic pathways, as evidence by increased phosphorylation of these proteins (Figure 4, B and C). Although R60L showed greater activation of p38 than the wild-type $G\alpha_{11}$ (Figure 4B), there was no significant difference between R60L and wild-type $G\alpha_{11}$ on the activation of pJNK (Figure 4C). Finally, we found no significant activation of the MARCKS (Figure 4D) or AKT (Figure 4E) pathways by either mutant $G\alpha_{11}$ compared with wild-type $G\alpha_{11}$.

Discussion

We identified a novel heterozygous germline mutation of *GNA11* encoding a p.R60L substitution in affected members of an extended family with autosomal dominant hypoparathyroidism and showed that this mutation, similar to activating mutations in the *CASR*, enhances downstream signaling pathways that have been associated with inhibition of synthesis and secretion of PTH. We confirmed the cosegregating pattern between the mutation and the disease phenotype through three generations (six affected patients). Our results thereby provide further evidence of a pathogenic role for G proteins that are coupled to parathyroid CaSRs in disorders of mineral metabolism (8, 9). To directly evaluate the effect of the R60L mutation on CaSR action, we expressed $G\alpha_{11}$ proteins in HEK293 cells that stable express the CaSR (HEK293-CaSR) and examined the responses of several signaling pathways to $[Ca^{2+}]_o$. Incubation of parathyroid and HEK293-CaSR cells with $[Ca^{2+}]_o$ stimulates phosphoinositol-specific phospholipase C (PI-PLC)-β, thereby leading to the accumulation of 1,2-sn-diacylglycerol (with activation of protein kinase C) and inositol 1,4,5-trisphosphate (with mo-

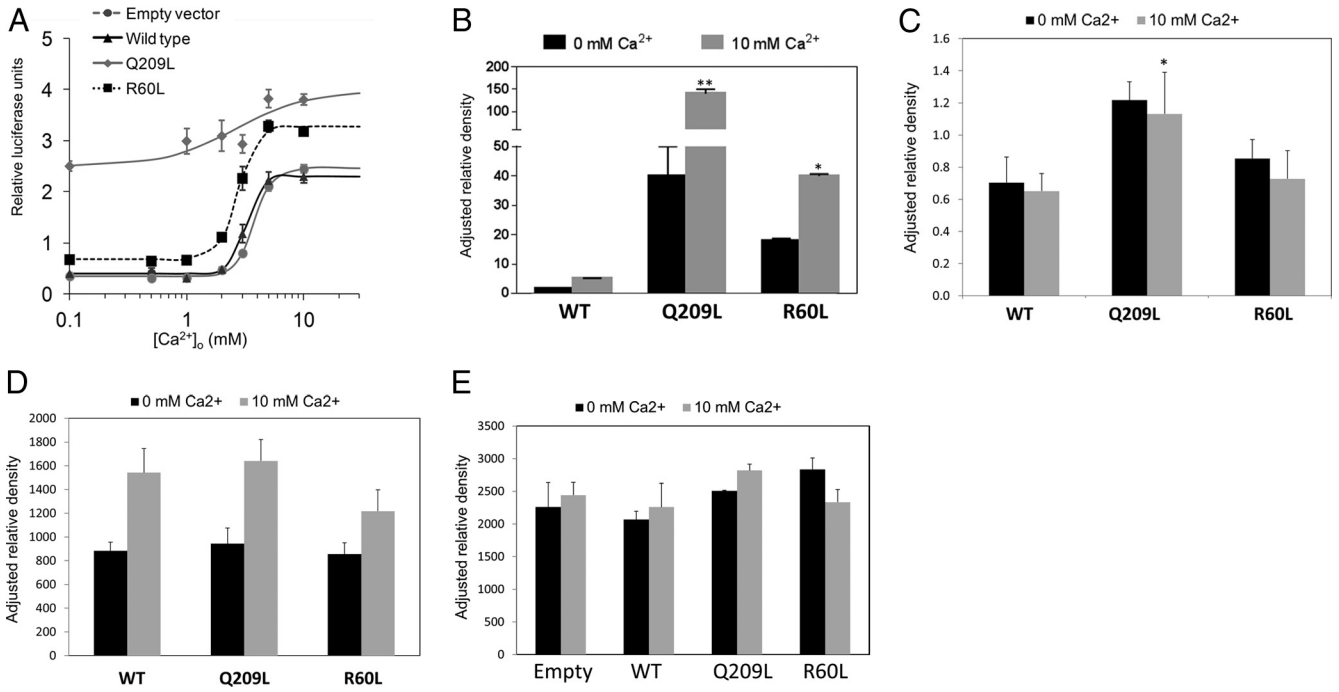

Figure 4. Downstream effectors of $G\alpha_{11}$ action. HEK293 cells stably expressing calcium-sensing receptors were transiently transfected with an empty expression plasmid vector or plasmids expressing $G\alpha_{11}$ cDNAs corresponding to the wild-type or mutant (R60L or Q209L) sequences. The data are expressed as arbitrary units and are shown as the mean (±SE) value from three experiments. Panel A shows the results of a SRE luciferase assay and depicts calcium-stimulated luciferase activity expressed under the control of the SRE promoter. The R60L mutant produced a leftward shift in the concentration-response curve, with significantly lower EC_{50} value than vector-only or wild type $G\alpha_{11}$ (see text). The Q209L mutant demonstrated constitutive activation of SRE promoter activity with modest increases in response to extracellular calcium. Panel B shows markedly greater phosphorylation of p38 with p.Q209L (**, $P < .005$ vs R60L or wild type) but only modestly (*, $P < .05$) greater phosphorylation by R60L compared with wild type $G\alpha_{11}$. Increased phosphorylation of JNK is seen with p.Q209L (*, $P < .05$) and weaker activation with p.R60L ($P = .07$) (panel C). No change in the phosphorylation of MARCKS (panel D) or AKT (panel E) is seen with either the $G\alpha_{11}$ p.R60L or the p.Q209L cDNA. WT, wild type.

bilization of calcium from intracellular stores). The generation of the second messengers inositol 1,4,5-trisphosphate and 1,2-*sn*-diacylglycerol appears to be a direct, G protein-mediated process, probably involving $G\alpha_{q/11}$ because this effect is not blocked by pertussis toxin (24). We found that the R60L mutation led to enhanced sensitivity of HEK293-CaSR cells to $[Ca^{2+}]_o$, with a leftward shift of the concentration-dependent accumulation of intracellular calcium that was similar to that produced by the $G\alpha_{11}$ Q209L gain-of-function mutation.

These results invited further comparison of the signaling properties of R60L with those of Q209L, and further analyses demonstrated important functional differences between the two mutant $G\alpha_{11}$ proteins. First, Q209L produced far greater activation of ERK1/2, which is stimulated through PI-PLC-β pathways. Second, Q209L showed greater activation of p38 and JNK than R60L, which requires interaction of $G\alpha_q$ and $G\alpha_{11}$ with the highly conserved guanine nucleotide exchange factor, Trio. Trio activates Rho- and Rac-regulated signaling pathways that act on JNK and p38 and thereby transduce proliferative and oncogenic signals from $G\alpha_q$ and $G\alpha_{11}$ independently of PI-PLC-β (25). And third, Q209L demonstrated constitutive activation of an SRE promoter-luciferase reporter, indicating enhanced downstream signaling through the MAPK pathway, whereas R60L produced only a moderately increased ligand-dependent activation compared with wild-type $G\alpha_{11}$ protein.

The reduced activity of R60L compared with Q209L provides a potential explanation for the survival of subjects who carry the R60L in their germline and also suggests a difference in the mechanism of the two mutations. Normally, G proteins are activated after interaction with ligand-bound heptahelical membrane receptors, which leads to release of GDP from the α-subunit. The subsequent binding of GTP leads to the dissociation of Gα-GTP from the $\beta\gamma$-dimer, with both subunits now able to regulate downstream effectors. The subsequent hydrolysis of GTP to GDP leads to the reassociation of the Gα-GDP and $\beta\gamma$ subunits, thereby ending the cycle of G protein activity. The oncogenic R183 and Q209 mutations in *GNA11* and *GNAQ* abrogate the intrinsic GTPase activity and thereby lead to constitutive activation. The greater effect of Q209 substitutions, as compared with R183 substitutions, has been proposed (23) to reflect differences in the ability of each mutant Gα protein to interact with regulator of G-protein signaling proteins, which function as GTPase activating proteins, as well as other downstream proteins (eg, Trio).

Based on molecular modeling, we propose an alternative mechanism to explain the weaker and less generalized activating effects of R60L. R60 is within an α-helical region immediately before linker 1, one of two linker sequences that position the GTPase domain near a second critical Gα region termed the helical domain, and together these two domains create a cleft in which bound guanine nucleotides are buried. The movement of the GTPase domain away from the helical domain is crucial for the opening process, and the linker regions are thought to act as hinges because they are relatively close together toward the phosphate end of the nucleotide. Current models suggest that interdomain interactions regulate both receptor-activated and basal GDP release rates (26). A salt bridge between Arg60 from the GTPase domain and Asp71 from the helical domain, the Arg-Asp pair, form multiple hydrogen bonds that stabilize the interaction between switch 1 and linker 1 in members of the $G\alpha_{q/11}$ family (16).

Our biochemical characterization of the R60L protein demonstrates that this replacement leads to a less robust gain of function relative to Q209L, which we propose is the result of enhanced release of GDP. Several lines of evidence support this proposal: first, experimental replacement of R60 in $G\alpha_q$ with a lysine residue markedly reduces sensitivity to inhibition by the cyclic depsipeptide YM-254890, which specifically inhibits GDP release from $G\alpha_q$ (16); second, biochemical characterization of three activated Gpa2 proteins identified in the yeast *Schizosaccharomyces pombe* demonstrated increased GDP-GTP exchange rates as the mechanism of activation of amino acid replacements I56S, L57P, and F62S, all of which are in the same region of the yeast protein as R60L (27); and third, a study of the transducin linker regions showed that converting the glycine residue at position 56 to proline led to an increase in the GDP-GTP exchange rate, presumably by altering the flexibility and conformation of the linker 1 region (21). Finally, while this work was in progress, missense mutations in *GNA11* were independently reported in other subjects with hypoparathyroidism. These mutations include R60C, suggesting that this is a critical residue for activation of $G\alpha_{11}$ (9) as well as R181Q near linker 2 (switch 1) (8), S211W in switch 2 (9), and F341L near the carboxyterminal region that interacts with heptahelical receptors (8). Only limited biochemical data were presented for these mutations, but these mutations are predicted to enhance agonist-dependent receptor-activated release of GDP and result in a mild phenotype. Similar germline mutations in the mouse, *Gna11* (I63V, *Dsk7*) and *Gnaq* (V179M, *Dsk1*) in linker 1 and 2, respectively, also cause a very mild phenotype in which dark skin, due to the stimulation of melanocytes, ap-

pears to be the principal consequence of these amino acid replacements (22).

The phenotype of the patients with the *GNA11* R60L mutation contrasts with the typical phenotype of patients with hypoparathyroidism owing to gain-of-function mutations of the *CASR*, who have mild hypocalcemia, hypomagnesemia, and in most cases, FEca (2, 3) and fractional excretion of magnesium (28). Urinary calcium excretion is greater than in patients with other forms of hypoparathyroidism because of expression of the activated CaSR in the thick ascending limb of the nephron reduces reabsorption of calcium (3). Clinically, hypercalciuria increases the risk for renal complications, including nephrocalcinosis, nephrolithiasis, and impaired renal function. By contrast, hypercalciuria is not a prominent clinical feature in the affected patients in this kindred (Table 1) or in the two unrelated patients with sporadic hypoparathyroidism due to *GNA11* mutations (R181Q and Phe341Leu) recently described by Nesbit et al (8). These observations imply that *GNA11* mutations exert less effect in the distal tubule than activating mutations of the CaSR. One possible explanation for this discrepancy is stoichiometry: although $G\alpha_{11}$ is the predominant member of the $G_{q/11}$ family in the parathyroid cell (8, 29), $G\alpha_q$ and $G\alpha_{14}$ are more highly expressed in the kidney and can also interact with the CaSR (26). It is also possible that CaSR-dependent inhibition of calcium reabsorption in the kidney occurs through signaling pathways that use members of the $G_{i/o}$ family, which can also couple with CaSRs (24, 30). Comprehensive studies of greater numbers of patients with different gain-of-function mutations in *GNA11* will be required to answer this question more fully, however.

Finally, we note that the affected patients in the family we describe here had short stature. Poor growth is not a typical consequence of germline activating mutations of *CASR* in humans or the *Nuf* mouse, in which an activating *Casr* mutation reproduces many of the findings in autosomal dominant hypoparathyroidism (31). Interestingly, Stock et al (32) described a three-generation family in which autosomal dominant hypoparathyroidism segregated with short stature and premature osteoarthritis. A C-to-G transversion at nucleotide 1846 in the *CASR* gene was identified that predicted a L616V substitution in the first transmembrane domain of the CaSR; although this nucleotide change cosegregated with the phenotype, the L616V replacement did not affect the accumulation of inositol phosphates in response to extracellular calcium in transfected HEK293 cells (32). By contrast, loss-of-function mutations in the *CASR* have been shown to have profound effects on skeletal growth and development (33–35), indicating that the CaSR affects chondrogenesis (36).

Stimulation of $G_{q/11}$ in skeletal cells has been associated with impaired growth. For example, short stature is present in patients with Jansen metaphyseal dysplasia, in which missense mutations in *PTHR1* cause constitutive activation of the receptor (37–39) and activation of $G_{q/11}$ (as well as G_s) signaling pathways. In addition, *Dsk* mice that are double homozygotes for *Gna11* and *Gnaq* activating mutations are small, and increasing the number of mutated alleles causes a progressive and linear decrease in body length at 6 weeks of age (22). Similarly, postnatal dwarfism was associated with suppression of osteoblast differentiation in transgenic mice that overexpressed the constitutively active Q209L $G\alpha_q$ cDNA specifically in osteoblasts under the control of the type 1 collagen α1 chain promoter (40). G_q and G_{11} activate a variety of downstream signaling pathways, and of importance in bone, these G protein coupled signals can activate MEK/ERK1/2 pathways. These pathways also propagate fibroblast growth factor receptor-3 (FGFR3) signals, and recent studies now show that the constitutive activation of MEK1 in chondrocytes causes signal transducer and activator of transcription-1(STAT1)-independent achondroplasia-like dwarfism in mice and rescues the fibroblast growth factor receptor-3-deficient mouse phenotype (41). These results indicate that MAPK activity is a negative regulator of bone growth and is essential for normal bone modeling and remodeling postnatally (42). Hence, it is tempting to speculate that the short stature observed in the affected subjects we describe here is related to the action of $G\alpha_{11}$ R60L on the maturation of the growth plate and/or the differentiation of the osteoblasts.

In conclusion, our data indicate that novel germline mutations in *GNA11* that result in a moderate gain of function can lead to a unique form of autosomal dominant hypoparathyroidism and suggest that short stature may be a unique expression of increased $G\alpha_{11}$ signaling in these patients.

Acknowledgments

We gratefully acknowledge Dr Teik Chye Ooi and Ms Maryjane Benton for assistance obtaining clinical and biochemical data on subjects reported here. This work was supported by

The content of this work is solely the responsibility of the authors and does not necessarily represent the official views of the National Institutes of Health.

Address all correspondence and requests for reprints to: Michael A. Levine, MD, Division of Endocrinology and Diabetes, The Children's Hospital of Philadelphia, 11 Northwest Tower, Suite 30, 34th and Civic Center Boulevard, Philadelphia, PA 19104. E-mail: levinem@chop.edu.

This work was supported in part by Grant R01DK079970 from the National Institute of Diabetes and Digestive and Kidney Diseases (to M.A.L.) and by the National Center for Research Resources and the National Center for Advancing Translational Sciences, National Institutes of Health, through Grant UL1TR000003 (to M.A.L.). Additional support for this study was provided by the Institutional Development Fund to the Center for Applied Genomics from The Children's Hospital of Philadelphia (to H.H.); and an Adele and Daniel Kubert donation (to H.H.).

Disclosure Summary: The authors have nothing to declare.

References

1. **Ahn TG, Antonarakis SE, Kronenberg HM, Igarashi T, Levine MA.** Familial isolated hypoparathyroidism: a molecular genetic analysis of 8 families with 23 affected persons. *Medicine (Baltimore)*. 1986; 65:73–81.
2. **Pollak MR, Brown EM, Estep HL, et al.** Autosomal dominant hypocalcaemia caused by a Ca(2+)-sensing receptor gene mutation. *Nat Genet*. 1994;8:303–307.
3. **Pearce SH, Williamson C, Kifor O, et al.** A familial syndrome of hypocalcemia with hypercalciuria due to mutations in the calcium-sensing receptor. *N Engl J Med*. 1996;335:1115–1122.
4. **Ding C, Buckingham B, Levine MA.** Familial isolated hypoparathyroidism caused by a mutation in the gene for the transcription factor GCMB. *J Clin Invest*. 2001;108:1215–1220.
5. **De Sanctis V, Soliman A, Fiscina B.** Hypoparathyroidism: from diagnosis to treatment. *Curr Opin Endocrinol Diabetes Obes*. 2012; 19:435–442.
6. **Heath D.** Familial hypocalcemia—not hypoparathyroidism. *N Engl J Med*. 1996;335:1144–1145.
7. **Yamamoto M, Akatsu T, Nagase T, Ogata E.** Comparison of hypocalcemic hypercalciuria between patients with idiopathic hypoparathyroidism and those with gain-of-function mutations in the calcium-sensing receptor: is it possible to differentiate the two disorders? *J Clin Endocrinol Metab*. 2000;85:4583–4591.
8. **Nesbit MA, Hannan FM, Howles SA, et al.** Mutations affecting G-protein subunit α11 in hypercalcemia and hypocalcemia. *N Engl J Med*. 2013;368:2476–2486.
9. **Mannstadt M, Harris M, Bravenboer B, et al.** Germline mutations affecting Gα11 in hypoparathyroidism. *N Engl J Med*. 2013;368: 2532–2534.
10. **Hunter AG, Heick H, Poznanski WJ, McLaine PN.** Autosomal dominant hypoparathyroidism: a proband with concurrent nephrogenic diabetes insipidus. *J Med Genet*. 1981;18:431–435.
11. **Li H, Durbin R.** Fast and accurate short read alignment with Burrows-Wheeler transform. *Bioinformatics*. 2009;25:1754–1760.
12. **McKenna A, Hanna M, Banks E, et al.** The Genome Analysis Toolkit: a MapReduce framework for analyzing next-generation DNA sequencing data. *Genome Res*. 2010;20:1297–1303.
13. **Wang K, Li M, Hakonarson H.** ANNOVAR: functional annotation of genetic variants from high-throughput sequencing data. *Nucleic Acids Res*. 2010;38:e164.
14. **Cingolani P, Platts A, Nguyen T, et al.** A program for annotating and predicting the effects of single nucleotide polymorphisms, SnpEff: SNPs in the genome of *Drosophila melanogaster* strain w1118; iso-2; iso-3. *Fly (Austin)*. 2012;6:80–92.
15. **Bramucci E, Paiardini A, Bossa F, Pascarella S.** PyMod: sequence similarity searches, multiple sequence-structure alignments, and homology modeling within PyMOL. *BMC Bioinformatics* 2012; 13(suppl 4):S2.
16. **Nishimura A, Kitano K, Takasaki J, et al.** Structural basis for the specific inhibition of heterotrimeric Gq protein by a small molecule. *Proc Natl Acad Sci USA*. 2010;107:13666–13671.
17. **Van Raamsdonk CD, Griewank KG, Crosby MB, et al.** Mutations in *GNA11* in uveal melanoma. *N Engl J Med*. 2010;363:2191–2199.
18. **Cheng Z, Garvin D, Paguio A, Stecha P, Wood K, Fan F.** Luciferase reporter assay system for deciphering GPCR pathways. *Curr Chem Genomics*. 2010;4:84–91.
19. **Motulsky HJ, Ransnas LA.** Fitting curves to data using nonlinear regression: a practical and nonmathematical review. *FASEB J*. 1987; 1:365–374.
20. **Kifor O, Kifor I, Brown EM.** Signal transduction in the parathyroid. *Curr Opin Nephrol Hypertens*. 2002;11:397–402.
21. **Majumdar S, Ramachandran S, Cerione RA.** Perturbing the linker regions of the α-subunit of transducin: a new class of constitutively active GTP-binding proteins. *J Biol Chem*. 2004;279:40137–40145.
22. **Van Raamsdonk CD, Barsh GS, Wakamatsu K, Ito S.** Independent regulation of hair and skin color by two G protein-coupled pathways. *Pigment Cell Melanoma Res*. 2009;22:819–826.
23. **Shirley MD, Tang H, Gallione CJ, et al.** Sturge-Weber syndrome and port-wine stains caused by somatic mutation in GNAQ. *N Engl J Med*. 2013;368:1971–1979.
24. **Kifor O, MacLeod RJ, Diaz R, et al.** Regulation of MAP kinase by calcium-sensing receptor in bovine parathyroid and CaR-transfected HEK293 cells. *Am J Physiol Renal Physiol*. 2001;280:F291–F302.
25. **Vaque JP, Dorsam RT, Feng X, et al.** A genome-wide RNAi screen reveals a Trio-regulated Rho GTPase circuitry transducing mitogenic signals initiated by G protein-coupled receptors. *Mol Cell*. 2013;49:94–108.
26. **Wettschureck N, Offermanns S.** Mammalian G proteins and their cell type specific functions. *Physiol Rev*. 2005;85:1159–1204.
27. **Ivey FD, Hoffman CS.** Direct activation of fission yeast adenylate cyclase by the Gpa2 Gα of the glucose signaling pathway. *Proc Natl Acad Sci USA*. 2005;102:6108–6113.
28. **Kinoshita Y, Hori M, Taguchi M, Watanabe S, Fukumoto S.** Functional activities of mutant calcium-sensing receptors determine clinical presentations in patients with autosomal dominant hypocalcemia. *J Clin Endocrinol Metab*. 2014;99:E363–E368.
29. **Varrault A, Pena MS, Goldsmith PK, Mithal A, Brown EM, Spiegel AM.** Expression of G protein α-subunits in bovine parathyroid. *Endocrinology*. 1995;136:4390–4396.
30. **Houillier P, Paillard M.** Calcium-sensing receptor and renal cation handling. *Nephrol Dial Transplant*. 2003;18:2467–2470.
31. **Hough TA, Bogani D, Cheeseman MT, et al.** Activating calcium-sensing receptor mutation in the mouse is associated with cataracts and ectopic calcification. *Proc Natl Acad Sci USA*. 2004;101: 13566–13571.
32. **Stock JL, Brown RS, Baron J, et al.** Autosomal dominant hypoparathyroidism associated with short stature and premature osteoarthritis. *J Clin Endocrinol Metab*. 1999;84:3036–3040.
33. **Chang W, Tu C, Chen TH, et al.** Expression and signal transduction of calcium-sensing receptors in cartilage and bone. *Endocrinology*. 1999;140:5883–5893.
34. **Chang W, Tu C, Pratt S, Chen TH, Shoback D.** Extracellular Ca(2+)-sensing receptors modulate matrix production and mineralization in chondrogenic RCJ3.1C5.18 cells. *Endocrinology*. 2002; 143:1467–1474.
35. **Wu S, Palese T, Mishra OP, Delivoria-Papadopoulos M, De Luca F.** Effects of Ca2+ sensing receptor activation in the growth plate. *FASEB J*. 2004;18:143–145.
36. **Chang W, Tu C, Chen TH, Bikle D, Shoback D.** The extracellular calcium-sensing receptor (CaSR) is a critical modulator of skeletal development. *Sci Signal*. 2008;1:ra1.
37. **Bastepe M, Raas-Rothschild A, Silver J, et al.** A form of Jansen's metaphyseal chondrodysplasia with limited metabolic and skeletal abnormalities is caused by a novel activating parathyroid hormone (PTH)/PTH-related peptide receptor mutation. *J Clin Endocrinol Metab*. 2004;89:3595–3600.

38. **Schipani E, Langman C, Hunzelman J, et al.** A novel parathyroid hormone (PTH)/PTH-related peptide receptor mutation in Jansen's metaphyseal chondrodysplasia. *J Clin Endocrinol Metab*. 1999;84:3052–3057.
39. **Schipani E, Langman CB, Parfitt AM, et al.** Constitutively activated receptors for parathyroid hormone and parathyroid hormone-related peptide in Jansen's metaphyseal chondrodysplasia. *N Engl J Med*. 1996;335:708–714.
40. **Ogata N, Kawaguchi H, Chung UI, Roth SI, Segre GV.** Continuous activation of Gαq in osteoblasts results in osteopenia through impaired osteoblast differentiation. *J Biol Chem*. 2007;282:35757–35764.
41. **Murakami S, Balmes G, McKinney S, Zhang Z, Givol D, de Crombrugghe B.** Constitutive activation of MEK1 in chondrocytes causes Stat1-independent achondroplasia-like dwarfism and rescues the Fgfr3-deficient mouse phenotype. *Genes Dev*. 2004;18:290–305.
42. **Guo J, Liu M, Yang D, et al.** Phospholipase C signaling via the parathyroid hormone (PTH)/PTH-related peptide receptor is essential for normal bone responses to PTH. *Endocrinology*. 2010;151:3502–3513.